

## Ab Initio Electronic Structure of the Rh–Rh Bond in Dirhodium Tetracarboxylate Complexes and Their Cations

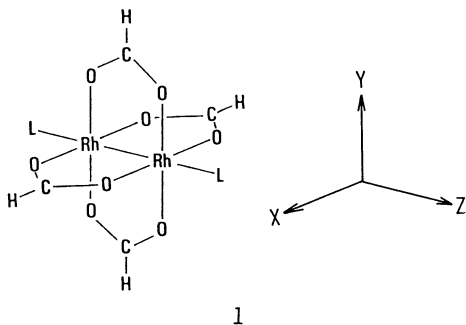
H. NAKATSUJI,\* Y. ONISHI, J. USHIO, and T. YONEZAWA

Received June 1, 1982

Electronic structures of dirhodium tetracarboxylate (DRTC) complexes,  $\text{Rh}_2(\text{O}_2\text{CH})_4\text{L}_2$ , and their cations with L absent and L =  $\text{OH}_2$ ,  $\text{NH}_3$ , and  $\text{PH}_3$ , have been calculated by the ab initio RHF and UHF methods. Several lower excited states of the cations were calculated individually by the UHF method, and the state level diagrams are reported. The electronic configuration of the ground state is calculated to be  $\delta^2\pi^4\pi^*\delta^*\sigma^1$  for the DRTC cations with L =  $\text{OH}_2$  and  $\text{PH}_3$ , while for L absent, the  $\delta^*$  orbital is the singly occupied (SO) MO. The results seem to be consistent with the ESR spectra, electronic spectra, and photoelectron spectra of the related compounds. The Rh–Rh bond is a weak single  $\sigma$  bond. The Rh–L bond is due to an electron-transfer interaction from L to Rh. The shortness of the Rh–Rh bonds in the DRTC complexes may be attributed to the existence of the bridging carboxylate ligands and the weakness of the Rh–Rh bond.

### Introduction

The electronic structures of dirhodium tetracarboxylate (DRTC) complexes,  $\text{Rh}_2(\text{O}_2\text{CR})_4\text{L}_2$  (**1**), have been the subject



of continuing interest, particularly with respect to the nature of the metal–metal bond and the mutual interactions of metal–metal and metal–ligand bonds. The Rh–Rh bond lengths in these complexes are from 2.386 to 2.486 Å,<sup>1–3</sup> considerably shorter than those in ordinary dirhodium complexes, 2.7–2.8 Å.<sup>4,5</sup> This abnormality was previously attributed by Cotton and co-workers<sup>2,5,6</sup> to a possible Rh–Rh triple bond with the electronic configuration  $\sigma^2\pi^4\delta^2\delta^*\sigma_n^2\sigma_n'^2$ , where  $\sigma_n$  and  $\sigma_n'$  are the rhodium nonbonding orbitals arising from the  $5p_z$  orbitals on each metal center. Dubicki and Martin<sup>7</sup> reported a single-bond configuration of  $\pi^4\sigma^2\delta^2\delta^*\pi^*$  by extended Hückel calculations and interpreted, on this basis, the variations in the electronic spectra upon changing the axial ligand L from  $\text{H}_2\text{O}$  to stronger donors. Norman and Kolari<sup>8</sup> carried out SCF– $X\alpha$ –SW calculations on  $\text{Rh}_2(\text{O}_2\text{CH})_4$  and  $\text{Rh}_2(\text{O}_2\text{CH})_4(\text{H}_2\text{O})_2$  and obtained the electronic configuration  $\sigma^2\pi^4\delta^2\pi^*\delta^*$ , which again suggests a single Rh–Rh bond. Their results for the corresponding cation radicals<sup>9</sup> have shown the same MO sequence of  $\sigma^2\pi^4\delta^2\pi^*\delta^*$ ; the singly occupied MO (SOMO) was predicted to be of  $\delta^*$  symmetry. A recent ESR study by Kawamura et al.<sup>10</sup> has shown, however, that

the SOMO's of the DRTC cations with phosphorus-centered ligands have  $\sigma$  symmetry.

In a previous preliminary paper,<sup>11</sup> we reported ab initio SCF MO calculations on the neutral DRTC complexes. The electronic configuration was calculated to be  $\pi^4\delta^2\pi^*\delta^*\sigma^2$  for L absent and L =  $\text{OH}_2$  and  $\text{NH}_3$  and  $\delta^2\pi^4\pi^*\delta^*\sigma^2$  for L =  $\text{PH}_3$ . The Rh–Rh bond is a single  $\sigma$  bond, and the HOMO is of  $\sigma$  symmetry. For L =  $\text{PH}_3$ , our results have agreed with the ESR results not only in the symmetry of the HOMO but also in the spin density distributions, i.e., a substantial Rh character of the HOMO. Bursten and Cotton<sup>12</sup> reported SCF– $X\alpha$ –SW calculations on the DRTC complex with L =  $\text{PH}_3$ . They also obtained a  $\sigma$  MO as the HOMO, but it localizes mostly on the axial phosphine ligands, in disagreement with the ESR experiment. For the DRTC complexes with L absent and L =  $\text{OH}_2$ , the MO sequence is different between the SCF– $X\alpha$  calculations<sup>8</sup> and the Hartree–Fock SCF calculations.<sup>11</sup>

Thus, it seems that the single-bond nature of the Rh–Rh bond in the DRTC complexes is now well established. However, uncertainties still remain on the natures (symmetries) of the ground electronic states of the cations of the DRTC complexes.

In this paper, we study several lower electronic states of the cations of the DRTC complexes with L absent and L =  $\text{OH}_2$ ,  $\text{NH}_3$ , and  $\text{PH}_3$ , by the ab initio UHF SCF MO method. We have calculated SCF solutions for each of the several lower states. We study (1) the symmetry of the ground electronic state of these cations, (2) the spin density distributions in these cations, (3) the electronic spectra of these cations (i.e., the transition energies and the oscillator strengths), (4) the ionization energies of the neutral DRTC complexes, and (5) the charge distributions and the natures of the Rh–Rh and Rh–L bonds in the DRTC complexes and their cations. We compare the present results with the experimental data now available. They are the spin density distributions estimated from the ESR experiments for the DRTC cations with L being the substituted phosphines  $\text{PX}_3$ ,<sup>10</sup> the electronic spectra of the DRTC cations with L =  $\text{OH}_2$ ,<sup>13,14</sup> and  $\text{PX}_3$ ,<sup>15</sup> and the photoelectron spectra

- (1) Christoph, G. G.; Koh, Y.-B. *J. Am. Chem. Soc.* **1979**, *101*, 1422.
- (2) Cotton, F. A.; DeBoer, B. G.; Laprade, M. D.; Pipal, J. R.; Ucko, D. A. *Acta Crystallogr., Sect. B* **1971**, *B27*, 1664.
- (3) Cotton, F. A.; Felthouse, T. R.; Klein, S. *Inorg. Chem.* **1981**, *20*, 3037.
- (4) Cotton, F. A. *Chem. Soc. Rev.* **1975**, *4*, 27.
- (5) Caulton, K. G.; Cotton, F. A. *J. Am. Chem. Soc.* **1971**, *93*, 1914.
- (6) Cotton, F. A.; DeBoer, B. G.; Laprade, M. D.; Pipal, J. R.; Ucko, D. A. *J. Am. Chem. Soc.* **1970**, *92*, 2926.
- (7) Dubicki, L.; Martin, R. L. *Inorg. Chem.* **1970**, *9*, 673.
- (8) Norman, J. G., Jr.; Kolari, H. J. *J. Am. Chem. Soc.* **1978**, *100*, 791.
- (9) Norman, J. G., Jr.; Renzoni, G. E.; Case, D. A. *J. Am. Chem. Soc.* **1979**, *101*, 5256.

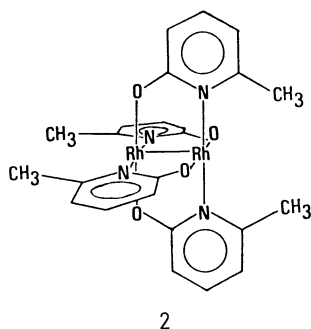
- (10) Kawamura, T.; Fukamachi, K.; Hayashida, S. *J. Chem. Soc., Chem. Commun.* **1979**, 945. Kawamura, T.; Fukamachi, K.; Sowa, T.; Hayashida, S.; Yonezawa, T. *J. Am. Chem. Soc.* **1981**, *103*, 364.
- (11) Nakatsuji, H.; Ushio, J.; Kanda, K.; Onishi, Y.; Kawamura, T.; Yonezawa, T. *Chem. Phys. Lett.* **1981**, *79*, 299.
- (12) Bursten, B. E.; Cotton, F. A. *Inorg. Chem.* **1981**, *20*, 3042.
- (13) Wilson, C. R.; Taube, H. *Inorg. Chem.* **1975**, *14*, 2776.
- (14) Cannon, R. D.; Powell, D. B.; Sarawek, K.; Stiilman, J. S. *J. Chem. Soc., Chem. Commun.* **1976**, 31.
- (15) Sowa, T.; Kawamura, T.; Shida, T.; Yonezawa, T. *Inorg. Chem.* **1983**, *22*, 56.

Table I. SCF Energies (eV) of the Neutral and Cation Species of the DRTC Complexes  $\text{Rh}_2(\text{O}_2\text{CH})_4\text{L}_2^{a-c}$ 

L absent			L = OH <sub>2</sub>			L = NH <sub>3</sub>		L = PH <sub>3</sub>		
state <sup>d</sup>	total energy		state <sup>d</sup>	total energy		state <sup>d</sup>	total energy single ζ	state <sup>d</sup>	total energy	
	double ζ	single ζ		double ζ	single ζ				double ζ	single ζ
neutral <sup>1</sup> A <sub>1g</sub>	0.0	0.0	neutral <sup>1</sup> A <sub>g</sub>	0.0	0.0	neutral <sup>1</sup> A <sub>g</sub>	0.0	neutral <sup>1</sup> A <sub>g</sub>	0.0	0.0
cation <sup>2</sup> B <sub>1u</sub> (δ*)	7.751	5.985	cation <sup>2</sup> A <sub>g</sub> (σ)	5.959	2.247	cation <sup>2</sup> A <sub>g</sub> (σ)	1.684	cation <sup>2</sup> A <sub>g</sub> (σ)	4.718	2.271
<sup>2</sup> A <sub>1g</sub> (σ)	8.321	4.009	<sup>2</sup> B <sub>1u</sub> (δ*)	6.443	4.557	<sup>2</sup> B <sub>g</sub> (π*)	4.063	<sup>2</sup> A <sub>u</sub> (δ*)	6.257	4.800
<sup>2</sup> A <sub>2u</sub> (σ*)	12.555	8.054	<sup>2</sup> B <sub>2g</sub> (π*)	7.267		<sup>2</sup> A <sub>u</sub> (δ*)	4.246	<sup>2</sup> B <sub>g</sub> (π*)	7.178	4.809
			<sup>4</sup> A <sub>g</sub> (δ*σσ*) <sup>e</sup>	7.289		<sup>2</sup> B <sub>1u</sub> (δ*)	6.589	<sup>2</sup> A <sub>u</sub> (π)	8.222	
			<sup>2</sup> B <sub>3u</sub> (π)	8.602				<sup>2</sup> B <sub>u</sub> (σ*)	8.412	6.775
			<sup>2</sup> A <sub>g</sub> (δ)	8.817				<sup>2</sup> B <sub>g</sub> (δ)	8.620	
			<sup>2</sup> B <sub>1u</sub> (σ*)	11.406						

<sup>a</sup> SCF energies are given relative to that of the neutral ground state. The double-ζ, single-ζ energies are as follows (au): -10 040.326 10, -10 036.560 08 for L absent; -10 190.366 92, -10 186.609 54 for L = OH<sub>2</sub>; -10 147.606 24 for L = NH<sub>3</sub>; -10 717.280 49, -10 713.702 42 for L = PH<sub>3</sub> (1 au = 627.5 kcal/mol). <sup>b</sup> 1 eV = 23.06 kcal/mol. <sup>c</sup> Note that the principal symmetry axis is parallel to the Rh-Rh bond for the DRTC complex with L absent but perpendicular to the Rh-Rh bond for the DRTC complexes with L = OH<sub>2</sub>, NH<sub>3</sub>, and PH<sub>3</sub>. <sup>d</sup> The greek letter shown in the parentheses denotes the symmetry of the singly occupied MO. <sup>e</sup> Note that this is a quartet spin state. <sup>f</sup> The energies of the <sup>2</sup>A<sub>g</sub>(σ) state calculated with the geometries of the neutral<sup>2</sup> and cation<sup>18c</sup> species are -10 190.147 93 and -10 190.169 29 au, respectively. Similar values for the <sup>2</sup>B<sub>1u</sub>(δ\*) state are -10 190.130 13 and -10 190.154 21 au, respectively.

of the related compound  $\text{Rh}_2(\text{mhpy})_4$  (**2**), where Hmhp is 6-methyl-2-hydroxypyridine.<sup>16</sup>



In the next section, we briefly explain the calculational details of the present ab initio SCF-MO studies. We then give the results related to the spectroscopic observables such as the ESR, UV, and photoelectron spectra and compare them with the experimental results now available. We study the charge distributions and the natures of the Rh-Rh and Rh-L bonds in the DRTC complexes and their cations. Conclusions of the present study are given in the last section.

### Calculational Details

Several lower electronic states of the cations of the DRTC complexes with L absent and L = OH<sub>2</sub>, NH<sub>3</sub>, and PH<sub>3</sub>, were calculated by the unrestricted Hartree-Fock (UHF) method. Independent SCF solutions were determined for several lower electronic states. For the neutral DRTC complexes, we have carried out the closed-shell restricted Hartree-Fock (RHF) calculations. The calculations were carried out with the use of a slightly modified version of the HONDOG program originally by King, Dupuis, and Rys.<sup>17</sup>

The geometries of the DRTC complexes are based on the experimental ones reported by Christoph and Koh;<sup>1</sup> the Rh-Rh, Rh-L lengths (in Å) are as follows for L absent and L = OH<sub>2</sub>, NH<sub>3</sub>, and PH<sub>3</sub>, respectively: 2.39, -; 2.39, 2.310; 2.403, 2.308; 2.449, 2.479. The geometry of the carboxylate ligand is from the X-ray structure of  $\text{Rh}_2(\text{O}_2\text{CCH}_3)_4(\text{H}_2\text{O})_2$ .<sup>2</sup> The geometries of the axial ligands, OH<sub>2</sub>, NH<sub>3</sub>, and PH<sub>3</sub>, were taken from the experimental data for the corresponding free molecules.<sup>18</sup> A *D*<sub>4h</sub> symmetry was assumed for the

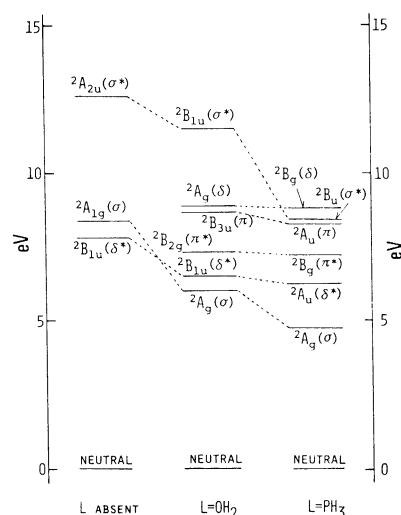


Figure 1. State level diagrams of the cations  $[\text{Rh}_2(\text{O}_2\text{CH})_4\text{L}_2]^+$  with L absent and L = OH<sub>2</sub> and PH<sub>3</sub> calculated with the double-ζ set. In parentheses is given the symmetry of the SOMO.

$\text{Rh}_2(\text{O}_2\text{CH})_4$  fragment. The DRTC with L = OH<sub>2</sub> was idealized to have a *D*<sub>2h</sub> symmetry while the DRTC's with L = NH<sub>3</sub> and PH<sub>3</sub> were idealized to have a *C*<sub>2h</sub> symmetry with the two NH<sub>3</sub> and PH<sub>3</sub> groups in an axially staggered form. The geometries were assumed to be the same for both neutral molecules and cations and for all of the lower electronic states of the cations. For the DRTC cations with L = OH<sub>2</sub>, we have also calculated some lower electronic states using the geometry reported for the cation itself.<sup>18c</sup> The purpose is to check the effect of geometrical change on the ordering of the σ and δ\* states.

Two kinds of basis sets were used. One is the minimal STO-3G level of basis set. For rhodium we have considered the inner-shell, 4d, 5s, and 5p AO's with the Slater exponents reported by Clementi et al.<sup>19</sup> The exponent of the 5p AO was assumed to be the same as that of the 5s AO. For the first-row atoms, the exponents are those reported by Stewart,<sup>20</sup> and for phosphorus, they are those of Roos et al.<sup>21</sup> In the second basis set, we have used double-ζ bases for the valence AO's of rhodium, i.e., 4d, 5s, and 5p AO's. They are those

- (16) Berry, M.; Garner, C. D.; Hillier, I. H.; MacDowell, A. A. *J. Chem. Soc., Chem. Commun.* **1980**, 494.  
 (17) King, H. F.; Dupuis, M.; Rys, J. "Program Library HONDOG"; Computer Center of the Institute for Molecular Science: Okazaki, Japan, 1979; Program No. 343. See also: Dupuis, M.; Rys, J.; King, H. F. *QCPE* **1977**, No. 338.  
 (18) (a) Herzberg, G. "Molecular Spectra and Molecular Structure"; Van Nostrand: Princeton, NJ, 1965; Vol. III. (b) Sutton, L. E. "Tables of Internuclear Distances and Configuration in Molecules and Ions"; Chemical Society: London, 1965. (c) Ziolkowski, J. J.; Moszner, M.; Glowiak, T. *J. Chem. Soc., Chem. Commun.* **1977**, 760.  
 (19) Clementi, E.; Raimondi, D. L.; Reinhardt, W. P. *J. Chem. Phys.* **1967**, *47*, 1300.  
 (20) Stewart, R. F. *J. Chem. Phys.* **1970**, *52*, 431.  
 (21) Roos, B.; Siegbahn, P. *Theor. Chim. Acta* **1970**, *17*, 199.

of Clementi et al.<sup>22</sup> For the other AO's, we have used the same single- $\zeta$  basis as above. We have denoted these two kinds of basis sets as the single- $\zeta$  set and the double- $\zeta$  set, respectively.

Since the double- $\zeta$  set is more reliable, especially for the energetic arguments, than the single- $\zeta$  set, we have based our energetic discussions on the results of the double- $\zeta$  set. The calculations with the single- $\zeta$  set were used for the analysis of charge distributions.

### Results on the Spectroscopic Observables

In this section we first show the results related to the spectroscopic observables and compare them with the experimental results now available. They are the results of the ESR, UV, and photoelectron spectra.

Table I shows the SCF energies of the neutral and cationic species of the DRTC complexes. The energy of each state of the cation was calculated independently by the UHF method. Figure 1 shows the state-level diagram of the DRTC cations. It shows the energy of the cation relative to the RHF energy of the corresponding neutral species. The symmetry of the singly occupied (SO) MO is shown in parentheses. Since the energy calculated by the double- $\zeta$  set seems to be more reliable than that of the single- $\zeta$  set, as seen from the ionization potential data shown below, we have selected only the results of the double- $\zeta$  set from Table I.

For the DRTC cation with L absent, the ground state was calculated to be of  $\delta^*$  symmetry. The energy difference between the  $\delta^*$  and  $\sigma$  states was calculated to be 0.57 eV (13.1 kcal/mol). However, for the cations with L = OH<sub>2</sub> and PH<sub>3</sub>, the state of  $\sigma$  symmetry was calculated to be the ground state. From the state-level diagram, the ground electronic configuration may be written as  $\delta^2\pi^4\pi^*\delta^*2\sigma^1$ . For the DRTC cation with L = OH<sub>2</sub>, the energy of the  ${}^2B_{1u}(\delta^*)$  state was calculated to be higher than that of the  ${}^2A_g(\sigma)$  state by 0.48 eV (11.2 kcal/mol). Comparisons with the spectroscopic data shown below seem also to support this result. Note, however, that the present result for L = OH<sub>2</sub> is different from that of the X $\alpha$ -SW calculations, which showed the electronic configuration to be  $\sigma^2\pi^4\delta^2\pi^*\delta^*1$ , predicting the SOMO to be of  $\delta^*$  symmetry. For the DRTC cation with L = PH<sub>3</sub>, the  ${}^2A_u(\delta^*)$  state was calculated to be higher than the  ${}^2A_g(\sigma)$  state by 1.54 eV (35.5 kcal/mol), so that the SOMO of the ground state is predicted unambiguously to be of  $\sigma$  symmetry. A recent ESR study by Kawamura et al.<sup>10</sup> has shown that the SOMO of the DRTC cations with phosphorus-centered ligands have  $\sigma$  symmetry. Our result is consistent with this observation.

For the DRTC cation with L = OH<sub>2</sub>, we have examined further the state ordering by ab initio calculations based on the geometry observed for the cation itself.<sup>18c</sup> The resultant ordering was however the same; the  ${}^2A_g(\sigma)$  state was calculated to be lower than the  ${}^2B_{1u}(\sigma^*)$  state by 0.41 eV (9.5 kcal/mol). Thus, a possibility of level crossing during the relaxation of the geometry from the vertical ionized state is negated. As shown in footnote f of Table I, the energy of the geometrical relaxation from the vertical state was calculated to be 0.60 eV (14 kcal/mol) and 0.66 eV (15 kcal/mol) for the  ${}^2A_g(\sigma)$  and  ${}^2B_{1u}(\delta^*)$  states, respectively.

The experimental geometry of the DRTC cation with L = OH<sub>2</sub> is different from that of the neutral species in especially the Rh-Rh and Rh-OH<sub>2</sub> lengths.<sup>18c</sup> The Rh-Rh and Rh-OH<sub>2</sub> lengths of the cation are shorter by 0.069 and 0.089 Å, respectively, than those of the neutral species. The  $\delta^*$  MO of the DRTC with L = OH<sub>2</sub> is weakly antibonding between the two Rh atoms and nonbonding between the Rh and OH<sub>2</sub>. Thus, the shortening of the Rh-Rh bond seems to agree with the assignment of the  $\delta^*$  MO as the SOMO of the cation, but the shortening of the Rh-OH<sub>2</sub> bond is not explained. Though a contraction of atomic radius of Rh is expected due to an

Table II. Diagonal Elements of the Spin Density Matrices of Rh<sub>2</sub>(O<sub>2</sub>CH)<sub>4</sub>L<sub>2</sub><sup>+</sup> Compared with the ESR Estimates<sup>a</sup>

site	AO	theor <sup>b</sup> diag elements of spin density matrices			ESR <sup>a</sup> estimate of odd-electron density
		L = OH <sub>2</sub>	L = NH <sub>3</sub>	L = PH <sub>3</sub>	
Rh	4d <sub>z<sup>2</sup></sub>	0.439	0.414	0.386	0.3-0.7
	5s	0.039	0.031	0.017	0.02-0.06
	5p <sub>z</sub>	0.054	0.071	0.101	
axial ligand L	ns	0.001	-0.001	-0.002	0.038-0.077
	np <sub>z</sub>	-0.002	-0.000	-0.007	0.09-0.14
	nd <sub>z<sup>2</sup></sub>			0.000	
	1s(H)	0.002	0.000	0.000	
maximum in carboxylate		-0.011	-0.009	-0.010	

<sup>a</sup> The ESR data were obtained for Rh<sub>2</sub>(O<sub>2</sub>CR)<sub>4</sub>(PY<sub>3</sub>)<sub>2</sub><sup>+</sup> (R = C<sub>2</sub>H<sub>5</sub>, CF<sub>3</sub>; PY<sub>3</sub> = PPh<sub>3</sub>, P(OPh)<sub>3</sub>, P(OCH<sub>2</sub>)<sub>3</sub>CC<sub>2</sub>H<sub>5</sub>).<sup>10</sup> <sup>b</sup> Data obtained with the single- $\zeta$  calculations.

increased positive charge on Rh, a larger change in the Rh-OH<sub>2</sub> length than in the Rh-Rh length seems to be difficult to be explained, though Norman et al. has given some account for that.<sup>9</sup> On the other hand, the  $\sigma$  MO is bonding between the two Rh atoms but antibonding between the Rh and OH<sub>2</sub> (see Figure 6 below). Thus, the observed shortening of the Rh-Rh length seems not to agree with the present assignment of the  $\sigma$  MO as the SOMO, but the shortening of the Rh-OH<sub>2</sub> length *does support* the present result. As Norman et al.<sup>8</sup> and our results<sup>11</sup> indicate, the Rh-Rh bond is a weak single bond so that its length depends rather sensitively on the environment, especially the nature of the ligands. Therefore, we believe that a large change in Rh-OH<sub>2</sub> distance is a more direct indicator of the electronic state of the cation than a change in the Rh-Rh length. Though an ab initio *full* geometry optimization of the cation in the  $\sigma$  and  $\delta^*$  states would resolve this problem, it is too time consuming to be realistic.

In Figure 1, the shift of the energy level of the cation with changing L absent and L = OH<sub>2</sub> and PH<sub>3</sub> reflects the natures and the strength of the interaction between the Rh-Rh bond and the ligand. As shown previously<sup>8,11</sup> and will be described below, the interaction between Rh and L is mainly the donation of the  $\sigma$ -lone-pair electrons of L to the vacant  $n\sigma$  and  $n\sigma^*$  MO's of Rh. Since both  $\sigma$  and  $\sigma^*$  MO's are antibonding between Rh and L, the stronger the Rh-L interaction is, the higher are the  $\sigma$  and  $\sigma^*$  MO levels. Thus, in the order of L absent, L = OH<sub>2</sub>, and L = PH<sub>3</sub>, the levels of the  $\sigma$  and  $\sigma^*$  states of the cation are lowered. Between L absent and L = OH<sub>2</sub>, a crossing of  $\sigma$  and  $\delta^*$  levels occurs. Since the interactions between the MO's of the DRTC and L with the symmetries other than  $\sigma$  are weak, the  $\delta$ ,  $\delta^*$ ,  $\pi$ , and  $\pi^*$  states are not affected as much as the  $\sigma$  and  $\sigma^*$  states.

Table II shows the diagonal elements of the spin density matrices obtained for the ground  $\Sigma$ -state of the DRTC cations. The ESR data may be compared with the present result for L = PH<sub>3</sub>. The present results agree well with the ESR estimates, though the 3s component of the phosphorus is smaller. The SCF-X $\alpha$ -SW calculation<sup>12</sup> on the neutral DRTC complex with L = PH<sub>3</sub> also predicted the SOMO of  $\sigma$  symmetry for its cation radical. However, the spin density distribution due to this SOMO lies 65% on PH<sub>3</sub>, 31% on Rh, and 4% on (O<sub>2</sub>CH)<sub>4</sub>; that is, it is largely localized on PH<sub>3</sub> in disagreement with experiment. In Table II we have also shown the spin density matrices of the cations with L = OH<sub>2</sub> and NH<sub>3</sub>. Though these numbers were all obtained from the single- $\zeta$  calculations, the results of the double- $\zeta$  basis were parallel to these. Note that, in the  $\delta^*$  state, the hfs constants are due to a spin-polarization mechanism.<sup>23</sup>

(22) Clementi, E.; Roetti, C. "Atomic Data and Nuclear Data Tables"; Academic Press: New York, 1974.

(23) Nakatsuji, H.; Kato, H.; Yonezawa, T. *J. Chem. Phys.* **1969**, *51*, 3175.

Table III. Electronic Spectrum of  $\text{Rh}_2(\text{O}_2\text{CR})_4(\text{H}_2\text{O})_2^+$ 

theor <sup>a</sup>			exptl <sup>b</sup>				
$D_{2h}$ transition	type	selection rule	$\text{Rh}_2(\text{O}_2\text{CH})_4(\text{H}_2\text{O})_2^+$		$\text{Rh}_2(\text{O}_2\text{CCH}_3)_4(\text{H}_2\text{O})_2^+$		
			transition energy, eV	oscillator strength	transition energy, eV	oscillator strength <sup>c</sup>	molar absorptivity, <sup>b</sup> $\text{M}^{-1} \text{cm}^{-1}$
$^2A_g(\sigma)$ Ground State							
$^2A_g \rightarrow ^2B_{1u}$	$\delta^* \rightarrow \sigma$	$z$ (weak)	0.48	$1.78 \times 10^{-8}$			
$^2A_g \rightarrow ^2B_{2g}$	$\pi^* \rightarrow \sigma$	forbidden	1.31	0.0	1.64	$4 \times 10^{-3}$	308
$^2A_g \rightarrow ^2B_{3u}$	$\pi \rightarrow \sigma$	$x, y$	2.64	$0.88 \times 10^{-3}$	2.41	$5 \times 10^{-3}$	298
$^2A_g \rightarrow ^2A_g$	$\delta \rightarrow \sigma$	forbidden	2.86	0.0	(3.1) <sup>d</sup>	(0.02) <sup>d</sup>	(800) <sup>d</sup>
$^2A_g \rightarrow ^2B_{1u}$	$\sigma \rightarrow \sigma^*$	$z$	5.45	0.506	5.72	...	11900
$^2B_{1u}(\delta^*)$ Ground State							
$^2B_{1u} \rightarrow ^2A_g$	$\sigma \rightarrow \delta^*$	$z$ (weak)	-0.48	$1.79 \times 10^{-8}$			
$^2B_{1u} \rightarrow ^2B_{2g}$	$\pi^* \rightarrow \delta^*$	$x, y$	0.82	$5.96 \times 10^{-5}$			
$^2B_{1u} \rightarrow ^2B_{3u}$	$\pi \rightarrow \delta^*$	forbidden	2.16	0.0			
$^2B_{1u} \rightarrow ^2A_g$	$\delta \rightarrow \delta^*$	$z$	2.37	0.928			
$^2B_{1u} \rightarrow ^2B_{1u}$	$\delta^* \rightarrow \sigma^*$	forbidden	4.96	0.0			
$^2B_{1u} \rightarrow ^2A_g$	$\sigma \rightarrow \sigma^*$	$z$	...	large			

<sup>a</sup> The results of the double- $\zeta$  set are shown. <sup>b</sup> In 1 M  $\text{CF}_3\text{SO}_3\text{H}$ .<sup>13</sup> <sup>c</sup> Calculated from the experimental data.<sup>13</sup> <sup>d</sup> In 0.02 M  $\text{Cl}^-$  in 1 M  $\text{HClO}_4$ .<sup>14</sup>

In Figure 2, we have shown the contour maps of the  $\sigma$  MO's of the DRTC cations  $[\text{Rh}_2(\text{O}_2\text{CH})_4(\text{H}_2\text{O})_2]^+$  and  $[\text{Rh}_2(\text{O}_2\text{CH})_4(\text{PH}_3)_2]^+$  in the ground state. We see that, though the MO's extend over all the molecules, the dominant parts are largely localized near the regions of the Rh-Rh and Rh-L bonds. They show a typical bonding pattern between the two Rh atoms and an antibonding pattern between Rh and ligand L.

Tables III and IV show the transition energies and the oscillator strengths for the electronic spectra of the DRTC cations with  $L = \text{OH}_2$  and  $\text{PH}_3$ , respectively. The theoretical transition energy is the so-called  $\Delta\text{SCF}$  value, i.e., the difference of the SCF energy for each state. The transition moment was calculated with the use of the corresponding orbital transformation<sup>24</sup> of the orbitals to minimize the number of overlaps between the MO's of different UHF solutions. The experimental transition energies are those of Wilson et al.,<sup>13</sup> Cannon et al.,<sup>14</sup> and Kawamura et al.<sup>15</sup> The experimental values of the oscillator strengths were calculated from the spectra given in the literature by using the approximation  $\int \epsilon(\tilde{\nu}) d\tilde{\nu} = \epsilon_{\text{max}} \tilde{\nu}_{1/2}$ , where  $\tilde{\nu}_{1/2}$  is the half-width of the band.

For the DRTC cation with  $L = \text{OH}_2$ , we have examined two different assignments of the spectra, one based on the  $^2A_g(\sigma)$  ground state and the other on the  $^2B_{1u}(\delta^*)$  ground state, in order to see which assignment simulates more naturally the experimental spectra. In Table III, the results based on the  $^2A_g(\sigma)$  ground state are given in the top section and the results based on the  $^2B_{1u}(\delta^*)$  ground state in the bottom section. A weak band at 1.64 eV appears only in the spectrum of the cation and not in the spectrum of the neutral species, so it is regarded as the transition from the doubly occupied orbital to the SOMO. We assign this band to the  $\pi^* \rightarrow \sigma$  transition. Norman et al.<sup>9</sup> assigned this band to the  $\sigma \rightarrow \delta^*$  transition in which the  $\delta^*$  MO is the SOMO in their  $X\alpha$ -SW calculation. The observed transition at 2.41 eV may be assigned to the  $x$ - $y$ -polarized  $\pi \rightarrow \sigma$  transition. This is supported by the good agreements with the experiments in both the transition energy and the oscillator strength. From the existence of the analogous band at 2.1 eV in the spectrum of the neutral species,<sup>13,25</sup> Norman et al. assigned this band to the transition  $\pi^* \rightarrow \sigma^*$  ( $x$ - $y$  polarized) as for the neutral species. In the present study,

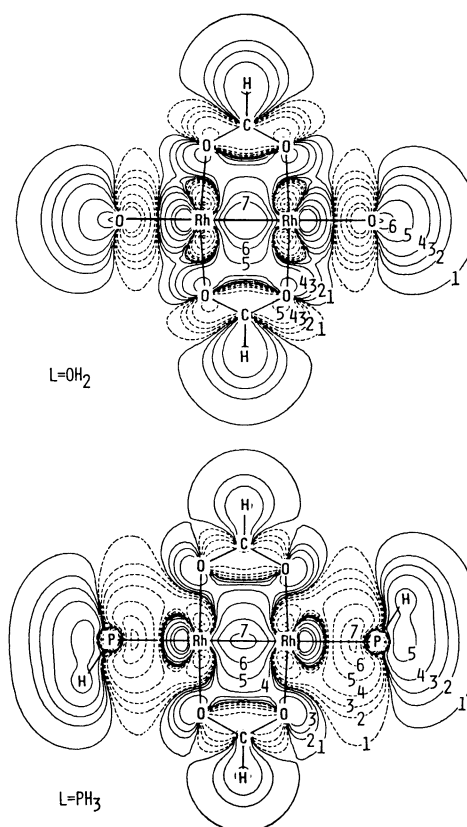


Figure 2. Contour maps of the  $\sigma$  MO of  $[\text{Rh}_2(\text{O}_2\text{CH})_4(\text{H}_2\text{O})_2]^+$  and  $[\text{Rh}_2(\text{O}_2\text{CH})_4(\text{PH}_3)_2]^+$  in the ground state ( $\Sigma$  state) calculated with the double- $\zeta$  set. The numbers 1-7 on contours correspond to the contour values 0.001, 0.005, 0.01, 0.02, 0.05, 0.1, and 0.14, respectively. The solid and broken lines correspond to the positive and negative signs of the MO, respectively.

we did not calculate the SCF solution for the  $\pi^* \rightarrow \sigma^*$  state, since it involves the multideterminantal open-shell configuration. The observed band at  $\sim 3.1$  eV seems doubtful because it appears only in solvents containing excess  $\text{Cl}^-$ .<sup>14</sup> So, no attempt was made to assign this band. The strong band at 5.72 eV is assigned to the  $\sigma \rightarrow \sigma^*$  transition. This assignment is confident from both the transition energy and its large absorptivity. (The experimental oscillator strength could not be estimated because of the lack of the spectrum in the literature). As shown later in Table IV, the  $\sigma \rightarrow \sigma^*$  transition

(24) Amos, A. T.; Hall, G. G. *Proc. R. Soc. London, Ser. A* **1961**, *263*, 483. King, H. F.; Stanton, R. E.; Kim, H.; Wyatt, R. E.; Parr, R. G. *J. Chem. Phys.* **1967**, *47*, 1936.

(25) Martin, D. S., Jr.; Webb, T. R.; Robbins, G. A.; Fanwick, P. E. *Inorg. Chem.* **1979**, *18*, 475.

Table IV. Electronic Spectrum of  $\text{Rh}_2(\text{O}_2\text{CR})_4(\text{PY}_3)_2^+$ 

		theor <sup>a</sup>			exptl <sup>b</sup>		
		$\text{Rh}_2(\text{O}_2\text{CH})_4(\text{PH}_3)_2^+$			$\text{Rh}_2(\text{O}_2\text{CC}_2\text{H}_5)_4(\text{PCy}_3)_2^+{}^c$		
$C_{2h}$ transition	type	selection rule	transition energy, eV	oscillator strength	transition energy, eV	oscillator strength <sup>d</sup>	molar absorptivity, $\text{M}^{-1} \text{cm}^{-1}$
${}^2A_g \rightarrow {}^2A_u$	$\delta^* \rightarrow \sigma$	$z$ (weak)	1.54	$2.25 \times 10^{-8}$			
${}^2A_g \rightarrow {}^2B_g$	$\pi^* \rightarrow \sigma$	forbidden	2.46	0.0			
${}^2A_g \rightarrow {}^2A_u$	$\pi \rightarrow \sigma$	$x, y$	3.50	$1.68 \times 10^{-3}$			
${}^2A_g \rightarrow {}^2B_g$	$\delta \rightarrow \sigma$	forbidden	3.90	0.0			
${}^2A_g \rightarrow {}^2B_u$	$\sigma \rightarrow \sigma^*$	$z$	3.69	0.599	2.89	0.6	46 000

<sup>a</sup> The results of the double- $\zeta$  set are shown. <sup>b</sup> In  $\text{CH}_2\text{Cl}_2$  containing 0.1 M  $n\text{-Bu}_4\text{NClO}_4$  at room temperature.<sup>15</sup> A different peak at 2.38 eV with oscillator strength 0.3 (molar absorptivity 20 000) was also observed. <sup>c</sup> Cy = cyclohexyl. <sup>d</sup> Calculated from the experimental data.<sup>15</sup>

Table V. Ionization Energies for  $\text{Rh}_2(\text{O}_2\text{CH})_4\text{L}_2$  with L Absent and L =  $\text{OH}_2$  and  $\text{PH}_3$  Compared with the Experimental Values for  $\text{Rh}_2(\text{mhp})_4$  (Hmhp = 6-Methyl-2-hydroxypyridine)

peak	exptl, <sup>a</sup> eV $\text{Rh}_2(\text{mhp})_4$	assignt of Berry et al. <sup>a</sup>	calcd from $\text{Rh}_2(\text{O}_2\text{CH})_4\text{L}_2$ <sup>b</sup>					
			L absent		L = $\text{OH}_2$		L = $\text{PH}_3$	
			assignt	$\Delta\text{SCF}$ , eV	assignt	$\Delta\text{SCF}$ , eV	assignt	$\Delta\text{SCF}$ , eV
A	6.49	$\delta^*$	$\delta^*$	7.75	$\sigma$	5.96	$\sigma$	4.72
B	7.25	$\pi^*$	$\pi^*$		$\pi^*$	7.27	$\pi^*$	7.18
C	7.64	mhp $\pi$						
D	8.00	$\delta$	$\sigma$	8.32	$\delta^*$	6.44	$\delta^*$	6.26
E	8.37	mhp $\pi$						
F	8.53	$\pi$	$\pi$		$\pi$	8.60	$\pi$	8.22
envelope		$\sigma$	$\delta$		$\delta$	8.82	$\delta$	8.62

<sup>a</sup> Reference 16. <sup>b</sup> The results of the double- $\zeta$  set are shown.

of the DRTC cation with L =  $\text{PX}_3$  also has a very large absorptivity.

In the bottom section of Table III, we have calculated the transition energies and the oscillator strengths, assuming the  ${}^2B_{1u}(\delta^*)$  state to be the ground state. In this case, a very strong band (oscillator strength 0.928) is expected theoretically at 2.37 eV, but such an absorption does not appear in the experimental spectrum. The strong band observed at 5.72 eV would again be assigned to the  $\sigma \rightarrow \sigma^*$  transition; the  $\delta^* \rightarrow \sigma^*$  transition calculated at 4.96 eV is forbidden by symmetry. The  $\sigma \rightarrow \sigma^*$  transition would show a large absorbance, though we could not obtain the corresponding SCF solution because this state involves multideterminants when the ground state is the  ${}^2B_{1u}(\delta^*)$  state. Thus, when we assume the  ${}^2B_{1u}(\delta^*)$  state as the ground state, we cannot explain the absence of a very strong band near 2.37 eV. The assignment of the  ${}^2A_g(\sigma)$  state to the ground state seems to be more natural.

For the cations of  $\text{Rh}_2(\text{O}_2\text{CR})_4(\text{PR}'_3)_2$ , Kawamura et al.<sup>15</sup> observed two strong peaks, band I at 1.77–2.44 eV and band II at 2.14–2.89 eV. For the complex with R = ethyl and R' = cyclohexyl, which is most similar to the DRTC complex with L =  $\text{PH}_3$ , bands I and II have maxima at 2.38 and 2.89 eV, respectively. The band at 2.89 eV was assigned to the  $\sigma \rightarrow \sigma^*$  transition from its dependence on ligands and from the similarity to the spectra of the neutral species. For the band at 2.38 eV, no assignment was reported. Table IV shows the present result for the DRTC cation with L =  $\text{PH}_3$ . The assignment of the  $\sigma \rightarrow \sigma^*$  transition seems reasonable because of the good agreement in the oscillator strength, though the calculated transition energy is larger than the observed value. The peak at 2.38 eV with the oscillator strength 0.3 ( $\epsilon = 20\,000$ ) seems not to be included in the transitions calculated here. The transitions calculated here are all weak except for the  $\sigma \rightarrow \sigma^*$  transition. Therefore, it will be the transition involving the ligand.

Table V shows the calculated ionization potentials of the DRTC complexes with L absent and L =  $\text{OH}_2$  and  $\text{PH}_3$ , compared with the photoelectron data reported by Berry et al.<sup>16</sup> for the bridged dirhodium complex  $\text{Rh}_2(\text{mhp})_4$  (2), where Hmhp is 6-methyl-2-hydroxypyridine. For the DRTC com-

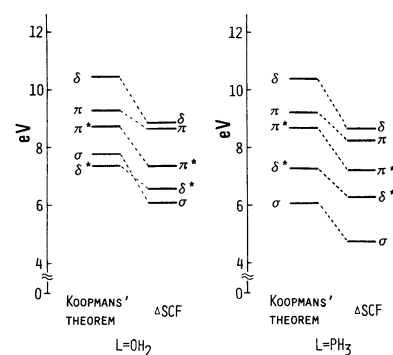
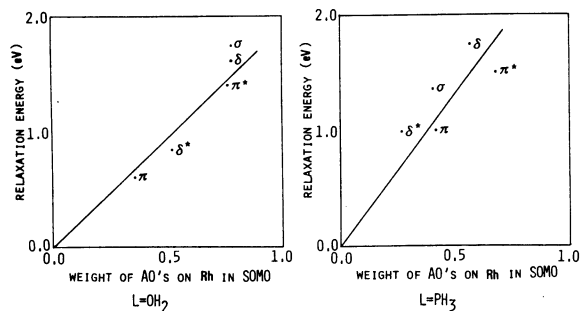
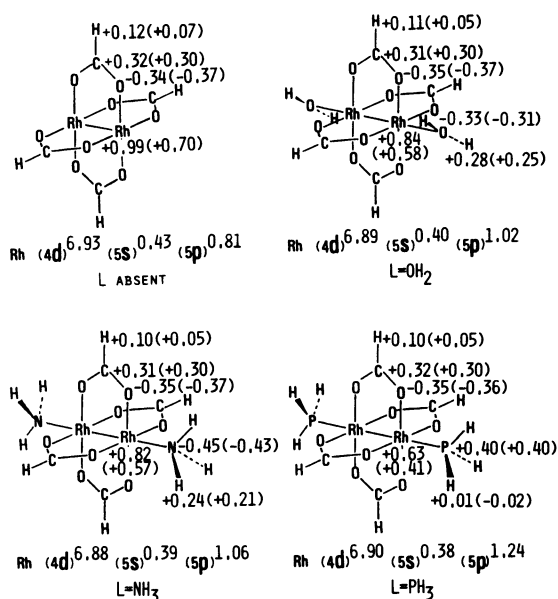


Figure 3. Ionization energies calculated from the Koopmans relaxation and the  $\Delta\text{SCF}$  method for  $\text{Rh}_2(\text{O}_2\text{CH})_4(\text{H}_2\text{O})_2$  and  $\text{Rh}_2(\text{O}_2\text{CH})_4(\text{PH}_3)_2$  (results of the double- $\zeta$  set).

plexes themselves, no photoelectron spectra are available. From spectral intensities, Berry assigned peaks B and F to the degenerate orbitals and peaks C and E to the  $\pi$  orbitals of the mhp ligand. Their further assignments were carried out with particular reference to the photoelectron spectrum of  $\text{Mo}_2(\text{mhp})_4$ . The present results of the ionization potential shown in Table V are the  $\Delta\text{SCF}$  values due to the double- $\zeta$  basis. Those due to the single- $\zeta$  basis are too small, as seen from Table I, to compare with experiments. The values obtained from the Koopmans approximation are generally too high (see Figure 2). In Table IV, the agreements between the experimental and theoretical values are good except for the peaks A and D. From the present calculation, the peaks A and D are assigned to the ionizations from either the  $\delta^*$  MO or the  $\sigma$  MO. The peaks B and F and the shoulder of the peak F are assigned to the ionizations from the  $\pi^*$ ,  $\pi$ , and  $\delta$  MO's, respectively. It is rather surprising that the ionization potentials calculated for  $\text{Rh}_2(\text{O}_2\text{CH})_4\text{L}_2$  show reasonable correspondence with those observed for  $\text{Rh}_2(\text{mhp})_4$  despite a large difference in the bridging ligands. This fact may be understood to suggest a similarity of the Rh–Rh bond between these complexes. The experiments for the DRTC complexes themselves are strongly expected.



**Figure 4.** Correlation between the relaxation energy and the weight of the AO's on Rh in the SOMO.



**Figure 5.** Net gross atomic charge for the  $\Sigma$  state of the DRTC cations calculated by the single- $\zeta$  basis. Those of the neutral species are given in parentheses.

It is interesting to examine the correspondence between the state level diagram of the cation and the MO level sequence of the neutral species. If the Koopmans relation is valid, the two levels should be identical. The difference between the Koopmans and  $\Delta$ SCF values is referred to as relaxation energy. Figure 3 shows the ionization energies obtained from the Koopmans relation and from the  $\Delta$ SCF method for  $L = \text{OH}_2$  and  $\text{PH}_3$ . Though the HOMO is  $\delta^*$  for the neutral DRTC complex with  $L = \text{OH}_2$ , the ground state of the cation has the SOMO of  $\sigma$  symmetry rather than  $\delta^*$  symmetry. This inversion is caused by the greater orbital relaxation in the  $\sigma$  MO than in the  $\delta^*$  MO. For the DRTC with  $L = \text{PH}_3$ , the HOMO of the neutral species is already of  $\sigma$  symmetry. As seen in Figure 2, the level sequence is the same from both the Koopmans relation and the  $\Delta$ SCF method.

It is generally recognized for transition-metal complexes that the orbital relaxation energy is larger for the ionization from the MO having larger metal character than from the MO largely localized on the ligands.<sup>26</sup> In Figure 4, we have plotted the relaxation energy vs. the weight of the metal AO's in the SOMO. We see a good parallelism between the two quantities for both the DRTC cations with  $L = \text{OH}_2$  and  $\text{PH}_3$ .

### Results on the General Electronic Structure

In this section, we want to clarify the nature of the Rh–Rh bond from some analyses of the electronic structures of the

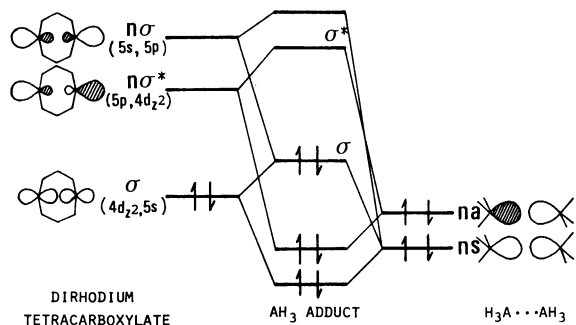


**Figure 6.** Nature of the charge-transfer interaction in DRTC complexes.

**Table VI.** MO Coefficients of the SOMO of the  $\Sigma$  State of  $\text{Rh}_2(\text{O}_2\text{CH})_4\text{L}_2^{+a}$

site	AO	L			
		absent	$\text{OH}_2$	$\text{NH}_3$	$\text{PH}_3$
Rh	$4d_{z^2}$	0.679	0.636	0.586	0.488
	5s	0.218	0.162	0.130	0.065
	$5p_z$	0.129	0.218	0.269	0.327
axial ligand L	ns		-0.078	-0.082	-0.143
	$np_z$		-0.106	-0.208	-0.233
	$nd_{z^2}$				0.013
	1s(H)		0.056	0.042	0.088
max in carboxylate		0.065	0.079	0.087	0.097

<sup>a</sup> Calculated with the single- $\zeta$  basis.

DRTC cations and their neutral species. In Figure 5, we have shown the net atomic charges of the DRTC cations having  $\sigma$  symmetry. They are the ground state except for the DRTC cation with L absent, for which the  $\delta^*$  state is calculated to be the ground state. The values in parentheses show the charges of the neutral species. These values were obtained from the single- $\zeta$  calculations. The charges of Rh in the  $\Sigma$  cations (neutral species) are +0.99 (+0.70), +0.84 (+0.58), +0.82 (+0.57), and +0.63 (+0.41) for L absent and  $L = \text{OH}_2$ ,  $\text{NH}_3$ , and  $\text{PH}_3$ , respectively, showing that the extent of the charge transfer is in the order of  $\text{OH}_2$ ,  $\text{NH}_3$ , and  $\text{PH}_3$ . The charge, 1+, of the cation is distributed over all the molecules, especially to Rh and H of the carboxylate ligand. This is also seen from the contour maps of the  $\sigma$  orbitals shown in Figure 2. The MO's extend from Rh to all over the carboxylate ligands. On the other hand, Figure 5 shows that the charge on the carboxylate ligand is hardly affected by a change in the axial ligand.

We note that the net atomic charges of the  $\Delta_u$  state (ground state) of the DRTC cation with L absent are very similar to those of the  $\Sigma$  state. Actually, the atomic charges on the carboxylate ligands are just the same as those of the  $\Sigma$  state, and the charge on Rh is +0.94 in the  $\Delta_u$  state instead of +0.99 in the  $\Sigma$  state.

In Figure 6, we have illustrated the orbital correlation diagram which explains the formation of the Rh–L bond. In the formation of the Rh–L bond, the charge transfer occurs from the lone pair of the axial ligand to the vacant nonbonding  $n\sigma^*$  (mainly composed of the  $5p_z$  and  $4d_{z^2}$  AO's of Rh) and  $n\sigma$  (mainly composed of the 5s and  $5p_z$  AO's of Rh) MO's of the DRTC. The occupied  $\sigma$  MO of the DRTC also interacts with the lone-pair MO's of the ligands, and the resultant Rh–Rh  $\sigma$  MO of the complex is antibonding between the Rh and the axial ligand. This is seen from Figure 2 and also from Table VI, where the MO coefficients of the SOMO of the  $\Sigma$  states are shown for various cations. Namely, the origin of the Rh–L bond is the  $\sigma$  transfer of the lone-pair electrons of L to the vacant MO's of Rh. The  $\pi$ -back-transfer interaction seems to be weak. The interaction increases in the order  $L = \text{OH}_2$ ,  $\text{NH}_3$ , and  $\text{PH}_3$  with decreasing order of the ionization

(26) Veillard, A.; Demuyneck, J. In "Modern Theoretical Chemistry"; Schaefer III, H. F., Ed.; Plenum Press: New York, 1977; Vol. 4.

**Table VII.** Change in the Valence AO Population of the Ground  $\Sigma$  State of the Cations of  $\text{Rh}_2(\text{O}_2\text{CH})_4\text{L}_2$  by Axial Ligand Addition<sup>a,b</sup>

site	AO	axial ligand L		
		$\text{OH}_2$	$\text{NH}_3$	$\text{PH}_3$
Rh	$4d_{x^2}, 4d_{y^2}, 4d_{xy}$	-0.015	-0.044	-0.040
	$4d_{z^2}$	-0.009	-0.001	+0.029
	$4d_{xz}, 4d_{yz}$	0.000	-0.001	-0.022
	5s	-0.036	-0.041	-0.058
	$5p_x, 5p_y$	+0.006	0.000	+0.023
axial ligand L	$5p_z$	+0.202	+0.249	+0.412
	ns	-0.057	-0.007	-0.184
	$np_z$	-0.053	-0.208	-0.179
	$np_x, np_y$	+0.041	+0.207	+0.163
	$nd_{x^2}, \dots, nd_{xz}$			+0.059
maximum in carboxylate	1s(H)	-0.098	-0.087	-0.093
		+0.017	+0.051	+0.040

<sup>a</sup> Relative to the cation of  $\text{Rh}_2(\text{O}_2\text{CH})_4$ . <sup>b</sup> Calculated with the single- $\zeta$  basis.

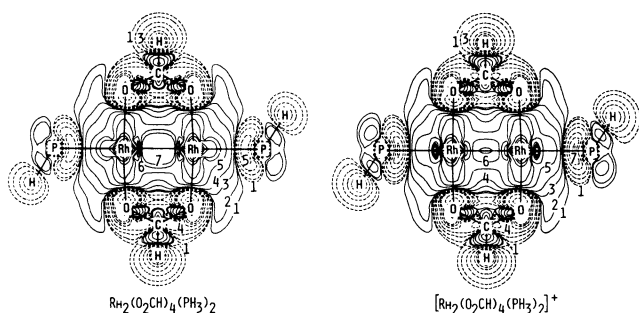


**Figure 7.** Density difference maps of the neutral molecule and cation of  $\text{Rh}_2(\text{O}_2\text{CH})_4(\text{PH}_3)_2$ . The numbers 1–10 on contours correspond to the contour values 0.001, 0.002, 0.005, 0.01, 0.02, 0.03, 0.04, 0.1, 0.2, and 0.5, respectively. The solid and broken lines correspond to an increase and decrease, respectively, from the density of the reference molecules (see eq 1).

potential of the lone-pair electrons: 12.6 eV for  $\text{OH}_2$ , 10.9 eV for  $\text{NH}_3$ , and 9.9 eV for  $\text{PH}_3$ .<sup>27</sup> As seen in Table VI, the coefficients of the axial ligand orbitals in the SOMO also increase in the same order. A decrease in the Rh–Rh bonding overlap when L is changed from  $\text{OH}_2$  to  $\text{PH}_3$  is seen in Figure 2. This is because an electron transfer from the lone pair of L into the Rh–Rh  $\sigma^*$  MO is larger for L =  $\text{PH}_3$  than for L =  $\text{OH}_2$ . The elongation of the Rh–Rh bond<sup>1</sup> in the order L =  $\text{OH}_2$ ,  $\text{NH}_3$ , and  $\text{PH}_3$  reflects this effect.

Table VII shows the change in the valence AO population of the ground state of the cation due to the axial ligand addition. The density increases largely in the  $5p_z$  AO of Rh and decreases in the ns and  $np_z$  AO's of the ligands as expected from the scheme of the charge-transfer interaction shown in Figure 6. Again the change is particularly large for the DRTC with L =  $\text{PH}_3$ . A smaller amount of back-transfer is seen in the  $2p_x$  and  $2p_y$  AO's of  $\text{OH}_2$  and  $\text{NH}_3$ . For  $\text{PH}_3$  it occurs in the  $3p_x$ ,  $3p_y$ , and  $3d_{z^2}$  AO's of phosphorus.

In Figure 7 we have shown the contour maps of the density differences of  $\text{Rh}_2(\text{O}_2\text{CH})_4(\text{PH}_3)_2$  and its cation defined by

$$\Delta\rho = \rho(\text{complex}) - \sum_i^2 \rho_i(\text{Rh}^{2+}) - \sum_i^4 \rho_i(\text{O}_2\text{CH}^-) - \sum_i^2 \rho_i(\text{PH}_3) \quad (1)$$

The densities were calculated by the double- $\zeta$  set. The electronic configuration of the Rh cation was chosen as  $(d_{xy})^2(d_{xz})^2(d_{yz})^2(d_{z^2})^1(d_{x^2-y^2})^0$  with the z axis along the two Rh atoms

and the x, y axes along the Rh–O bonds. The densities of the carboxylate anion and phosphine were calculated for the isolated molecules. The left-hand side of the figure is for the neutral species and the right-hand side for the cation. An accumulation of electron density near the center of the two Rh atoms shows the existence of the direct Rh–Rh bond. An electron transfer is seen from the  $\sigma$  lone pairs of the oxygens of the carboxylate anion to mainly the  $d_{x^2-y^2}$  AO's of Rh. This is an origin of the coordination of the carboxylate ligand to Rh atoms. The maps also show a transfer of the  $n\sigma$  lone-pair electrons of  $\text{PH}_3$  to the regions of the Rh–Rh bond. This is an origin of the coordination of  $\text{PH}_3$  to the DRTC complex as explained from the correlation diagram (Figure 6). Comparing the density for the cation with that of the neutral molecule, we see that an electron is ionized mostly from the region of the two Rh atoms. The decrease in the bond electron density due to the ionization suggests a weakening of the Rh–Rh bond in the cation.

The results of the present study seem to suggest that the Rh–Rh bonds in the DRTC complexes and their cations are weak, though there is certainly a direct Rh–Rh  $\sigma$  bond. That the  $\sigma$  MO lies at the HOMO or next to the HOMO means that the Rh–Rh bond is weak. For a stronger bond the  $\sigma$  MO should lie lower than the  $\pi$ ,  $\pi^*$ ,  $\delta$ , and  $\delta^*$  MO's. The contour map of the localized  $\sigma$  orbital shown previously<sup>11</sup> had also suggested a weakness of the Rh–Rh bond.

Now a question still remains. Why are the Rh–Rh bonds in the DRTC complexes so short? We guess that this is mainly due to the bridging carboxylate ligands. Since the Rh–Rh bond is weak as discussed above, the Rh–Rh distance can be changed by a relatively small perturbation. Experimental facts that seem to support this consideration are as follows: (1) The Rh–Rh distance in the DRTC complex is longer than the O...O distance of the carboxylate ligand. This is as if the two Rh atoms are pulled by the oxygens of the carboxylate ligands. (2) In the structures of the series of complexes  $\text{Rh}_2(\text{OAc})_4(\text{PPh}_3)_2$ ,<sup>4</sup>  $\text{Rh}_2(\text{OAc})_2(\text{dmg})_2(\text{PPh}_3)_2$ ,<sup>28</sup> and  $\text{Rh}_2(\text{dmg})_4(\text{PPh}_3)_2$ ,<sup>5,29</sup> where dmg is dimethylglyoximate, the Rh–Rh distance increases drastically as the bridging acetate ligands are replaced by the nonbridging dmg ligands, viz., 2.45, 2.62, 2.94 Å. Norman and Kolari<sup>8</sup> have given a similar opinion. According to Christoph et al.,<sup>30</sup> the repulsive steric effects of dmg ligands must also be borne in mind.

## Conclusion

Electronic structures of the dirhodium tetracarboxylate (DRTC) complexes  $\text{Rh}_2(\text{O}_2\text{CH})_4\text{L}_2$  and their cations with L absent and L =  $\text{OH}_2$ ,  $\text{NH}_3$ , and  $\text{PH}_3$  have been calculated by the ab initio RHF and UHF methods. Several lower excited states of the cations were also calculated individually by the UHF method, and the state level diagram is reported. The electronic configuration of the ground state was predicted to be  $\delta^2\pi^4\pi^*\delta^*2\sigma^1$  for the DRTC cations with L =  $\text{OH}_2$  and  $\text{PH}_3$ , while for L absent, the  $\delta^*$  orbital was calculated to be the SOMO. For the DRTC cation with L =  $\text{OH}_2$ , we have further considered the effect of the geometrical relaxation but obtained the same result. The change of the  $\sigma$  level with the change in the axial ligand is explained from the nature of the interaction between the DRTC complex and the axial ligand. We have examined our theoretical results by comparing with the ESR, UV, and photoelectron spectra of the related compounds. The spin density distribution calculated for the DRTC cation with L =  $\text{PH}_3$  agrees well with the ESR estimates of the related compounds. The electronic spectra of the cations

(27) Turner, D. W.; Baker, C.; Baker, A. D.; Brundle, C. R. "Molecular Photoelectron Spectroscopy"; Wiley: New York, 1970.

(28) Halpern, J.; Kimura, E.; Molin-Case, J.; Wong, C. S. *J. Chem. Soc. D* **1971**, 1207.

(29) Caulton, K. G.; Cotton, F. A. *J. Am. Chem. Soc.* **1969**, *91*, 6518.

(30) Christoph, G. G.; Halpern, J.; Khare, G. P.; Koh, Y.-B.; Romanowski, C. *Inorg. Chem.* **1981**, *20*, 3029.

$[\text{Rh}_2(\text{O}_2\text{CCH}_3)_4(\text{H}_2\text{O})_2]^+$  and  $[\text{Rh}_2(\text{O}_2\text{CC}_2\text{H}_5)_4(\text{PCy}_3)_2]^+$  (where Cy = cyclohexyl) are consistent with the present results for L = OH<sub>2</sub> and PH<sub>3</sub>, respectively. The assignments are different from those due to the X $\alpha$ -SW calculation. The photoelectron spectra of Rh<sub>2</sub>(mhp)<sub>4</sub>, with Hmhp being 6-methyl-2-hydroxypyridine, were also compared with the present result.

We have investigated the charge distributions and the natures of the Rh-Rh and Rh-L bonds. The origin of the Rh-L bond is mainly the transfer of the lone-pair electrons of the axial ligands to the empty nonbonding orbital on the Rh of the DRTC complex. The back-transfer interaction is small. The Rh-Rh bond is a weak single  $\sigma$  bond. This is reflected in the fact that the  $\Sigma$  level is the ground state or next to the ground state in the cations. We guess that the reason of the shortness of the Rh-Rh bond in the DRTC complexes is due to the existence of the bridging carboxylate ligand. As the Rh-Rh bond is weak, the distance is chiefly determined by the coordination distance of the carboxylate cage.

Finally, let us consider the role of electron correlation. Benard<sup>31</sup> has studied the effect of electron correlation for

molecules including a metal-metal bond, through the instability of a Hartree-Fock solution. He concluded that, though the electron correlation is very important for the description of a multiple metal-metal bond, it is less important for binuclear complexes that are without a metal-metal interaction or that display a single metal-metal bond.

**Acknowledgment.** We thank Dr. T. Kawamura for kindly showing us his experimental results on the electronic spectra of the DRTC cations with substituted phosphines prior to publication. The calculations were carried out with M-200 computers at the Institute for Molecular Science and at the Data Processing Center of Kyoto University. Part of this study was supported by a Grant-in-Aid for Scientific Research from the Japanese Ministry of Education, Science, and Culture.

**Registry No.** **1** (L absent), 33773-07-8; **1**<sup>+</sup> (L absent), 71767-77-6; **1** (L = OH<sub>2</sub>), 33700-44-6; **1**<sup>+</sup> (L = OH<sub>2</sub>), 72067-43-7; **1** (L = NH<sub>3</sub>), 15005-98-8; **1**<sup>+</sup> (L = NH<sub>3</sub>), 85185-76-8; **1** (L = PH<sub>3</sub>), 77965-51-6; **1**<sup>+</sup> (L = PH<sub>3</sub>), 85185-75-7.

---

(31) Benard, M. *J. Chem. Phys.* **1979**, *71*, 2546.